



Impacts of U and Inverted U-Bends on Vertical Gas-Liquid Two-Phase Fluids

Almabrok Abushanaf Almabrok

Petroleum Engineering Department, Faculty of Engineering- Sirte University, Sirte, Libya

Corresponding Author: Almabrok.Abushanaf@su.edu.ly

ARTICLE INFO

Article history:

Received 17 Feb 2023

Revised 5 March 2023

Accepted 9 March 2023

Available online:

4 May 2023

ABSTRACT

The current work is experimentally based which is conducted on the purpose of studying the impacts of U and inverted U-bends on gas/liquid behavior in a vertical upward and downward flow line. The main instruments used are wire mesh sensor (WMS) and liquid film probes. Both devices are installed at the top and bottom locations of upward and downward sections. Probability density functions (PDFs) and time traces of averaged void fraction are applied to reveal the flow behavior inside this configuration. It is very obvious from achieved results that the flow structure in the adjacent parts of the bends is significantly different from those apart away. These bends act on distribution of the flow and change it from uniform to ununiform in adjacent straight sections of the pipeline. This is attributed to the action of centrifugal and gravitational forces that generated by the bends. The results are further explained by analysis the reconstructed images obtained from Wire Mesh Sensor technique, and circumferential distribution of liquid film that measured by conductive film probes. The data of liquid film profile are consistent with PDFs and time traces data extracted by WMS.

2023 Sirte University, All rights are reserved

Keywords: Downward, Upward, 180° Bend, Film Thickness Probes, Wire Mesh Sensor

1. Introduction

Vertical pipes that arranged in a serpentine geometry are commonly used in numerous number of oil and gas production systems such as refineries. However,

many researchers are tending to investigate the flow behavior in such configuration in order to develop their design and avoid any issues that may occur. The knowledge of bend effects on flow structure is still insufficient.

A centrifugal and gravitational forces present in the bend are generating random flow fluctuations when it reaches the straight parts of the pipe. Such behavior could cause a dry spots on the internal surfaces of the tubes due to absence of a steady liquid phase. This in turn could create serious catastrophic events such as wall cracking of the tubes and overheating their internal surfaces. Hence, the early maintenance, shutdown of the equipment, and increasing the cost of operation will be the consequences.

Although, considerable investigations of gas-liquid flow behavior in vertical pipes, the majority of them were limited to a small internal diameter in upward orientation. Studies the impacts of U and inverted U-bends on the fluids flowing in large upward and downward pipes are still scarce. Except few researchers such as Abdulkadir et al. [1] who conducted their experimental work in a large diameter pipe of 127 mm.

Early studies are carried out by Alves [2] Oshinowo and Charles [3], and Usui et al. [4]. Later on, investigations reported by Azzi et al. [5], Azzi and Friedel [6], Spedding and Benard [7] and Shannak et al. [8] are published their work in a literature. As mentioned above, Abdulkadir et al. [1] measured the liquid film in 180° return bend using a large diameter (i.d. 127 mm). They discussed the behavior of churn and annular flows using electrical conductance tomography. They also used the conductance ring probes to measure the liquid film fraction, which installed before the bend, inside the bend and after the bend (i.e., at 45°, 90°, and 135° positions). They reported that, the values of film fraction for low liquid and high gas flow rates are notably higher in the straight section than that in the bend. They also stated that the behaviour of gas-liquid inside the bend affected by the generated gravitational and centrifugal forces.

2. Experimental Setup

The facility is constructed to clarify the impact of bends on flow behaviour in large serpentine pipes. Figures 1 to 4, respectively illustrate the main parts of test facility, top & bottom bends, liquid film probes and WMS. The length of vertical flow line is twenty meter with internal diameter of 4 inch. The upward and downward sections are arranged in parallel and connected together by U and inverted U-bends.

The facility comprises the test and separation parts, metering and fluid supply sections. Labview and delta-V are the data acquisition system that are applied to control the test facility and record the possible raw data. The gas and liquid flowrates are predetermined and mixed together in a T-shaped junction before entering the upward section of the test facility. The air and water are used as a working fluids which are flowing in the test loop (i.e., along upward and downward sections) to eventually reach a ventilation tank for separation. The separated liquid flows into a storage tank, while the gas vented into the surrounding environment. The main devices installed on the test facility are conductive film thickness probes and capacitance wire mesh sensor (WMS), as illustrated in Figures 3 and 4, respectively. Both devices are constructed at three locations of upward and downward sections. More information of wire mesh sensor are presented by Da Silva et al. [9].

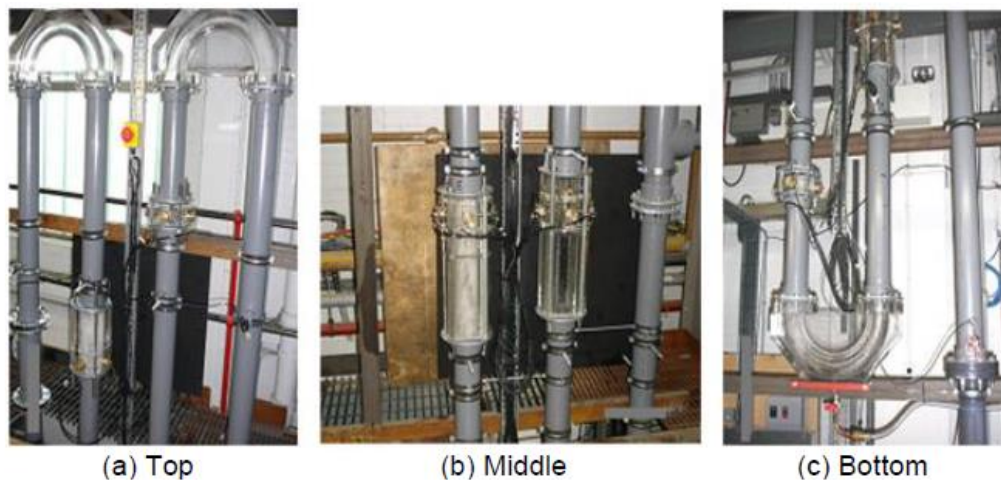


Figure 1: Three sections of experimental facility



Figure 2: Shape of bends

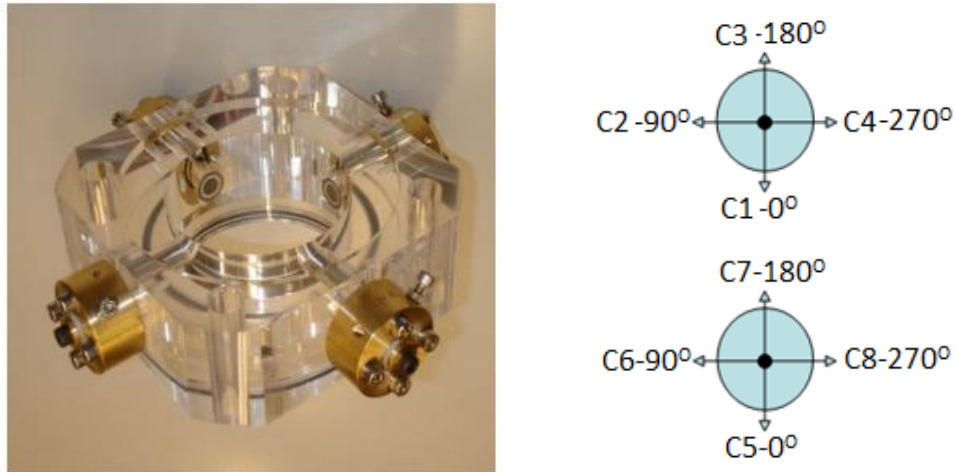


Figure 3: Circumferential distribution of the sensors inside the film probe

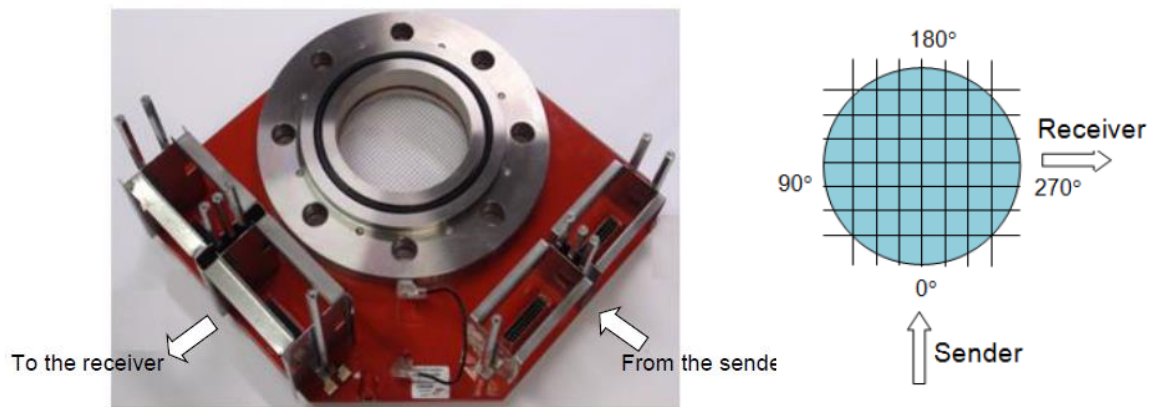


Figure 4: WMS and its cross-sectional area

For accurate results, the following steps need to be applied regularly before starting the experiments:

- A. The rig is first emptied and blown dry.
- B. The air flow is stopped to gain zero points of liquid film probes.
- C. The rig has to be fully filled by water to measure the maximum scale of liquid film probes.
- D. The water flow has to be put at a desired rate before injecting the air into the test section.
- E. The water flow has to be carefully adjusted to maintain the predetermined rate while the injected air is gradually increased until reach the desired rate.
- F. The water flow is adjusted accordingly.
- G. Eventually, the rig has to be emptied again and blown dry to measure the zero point of liquid film probes.

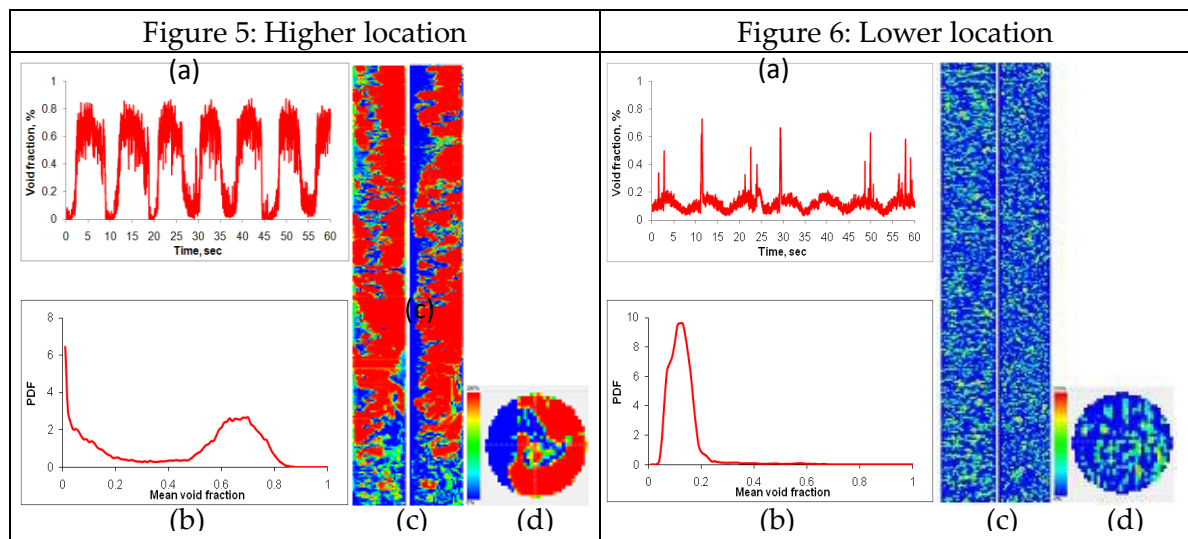
3. Results and Discussion

This study presents the results of liquid film and local distribution of gas void fraction at various locations of a vertical flow line. The data are achieved using probability density functions (PDFs) and cross-sectional distribution of gas void fraction which expected to give a deeper understanding about the impacts of 180° bend on the flow structure in a serpentine geometry.

3.1 Flow Structure Along Downward Section

Figures 5 and 6 are respectively, representing the flow structure at higher and lower locations of the downward orientation (namely, close to the top bend) for a relatively low gas velocity of 0.17 m/s and liquid velocity= 1.2 m/s. The measurement of time series at higher location of the pipeline shows wave fluctuations which is indicated that the flow pattern is intermittent, as illustrated in Figure 5 (a). The corresponding PDF data presented in Figure 5 (b) confirms that the flow characteristic is an intermittent with two peaks. As can be noted at the higher position (Figure 5 (c and d)), a huge wisps in the shape of objects accompanied by tails are distributed in different location of the pipe and entrained into the pipe center. On the other hand, some parts of the inner pipe surface are dry. Figure 5 (c) depicted the mixture structure in the cross section area of the pipe. Obviously, it is observed that most of liquid fraction is existed in 90 degree position (i.e., in the same direction of the top bend's outer curvature). This is due to action of centrifugal force generated by the higher bend. This bend expel the liquid phase into its outer curvature and consequently large quantity of liquid are accumulated on the same direction of the bend's outer curvature.

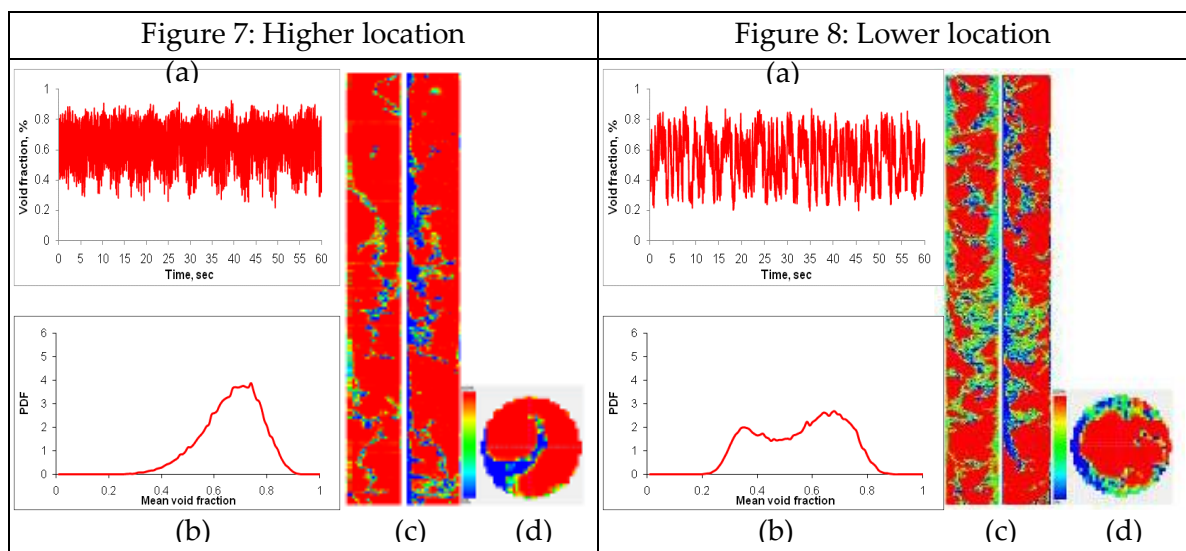
For the same conditions of gas and liquid velocities, different flow type is observed in the lower location (Figure 6 (a) & (b)). The distribution of the mixture in the cross section area is more symmetric with small bubbles dispersed in a liquid continuum which is indicated to bubbly flow regime.



Figures 5 & 6: (a) Time traces, (b) PDF, (c) cross-sectional view and (d) sliced stack image of void fraction at higher and lower locations of downward orientation, for gas velocity=0.17 m/s and liquid velocity=1.2 m/s

Figures 7 (a) and 8 (a) show the wave structure at the top and bottom locations, respectively. It can be noted from the plots that there are discrepancies of wave characteristics between both positions, this can be attributed to the impact of centrifugal force of top bend on distribution of gas void fraction. The action of the force led to create a huge oscillation in the mixture at the adjacent section of the bend (Figure 7 (a)). On the other hand, the identified flow type at the bottom location is slug (Figure 8 (a)). Analysis of PDF data at the top and bottom locations are also confirmed the results of time series. Figure 7 (b) shows flow instability accompanied by broad base of gas void fraction, for liquid and gas superficial velocities of 1.2 and 1.05 m/s, respectively. While, different structure of the flow regime (slug flow) is noted when it reached the bottom location of the pipe, as presented in Figure 8 (b). Again, the dissimilarity between the flow behaviour at the higher and lower locations is due to the impact of the centrifugal force of the top bend on the distributions of void fraction. This impact is notably stronger at the adjacent section of the top bend and reduced when the flow reached the bottom of the pipe. Figure 7 (c) and (d) are respectively, presented the cross-sectional view and sliced stack images as another approach to validate the results of time traces and PDFs. Figure 7 (c) and (d) depicts the flow imaging at the top location which is an asymmetrically distributed and accompanied by a huge droplets of liquid. These droplets are entrained in the centre of the pipe in Figures 7 (a) and 8 (a) show the wave structure at the top and bottom locations, respectively. It can be noted from the plots that there are discrepancies of wave characteristics between both positions, this can be attributed to the impact of centrifugal force of top bend on distribution of gas void

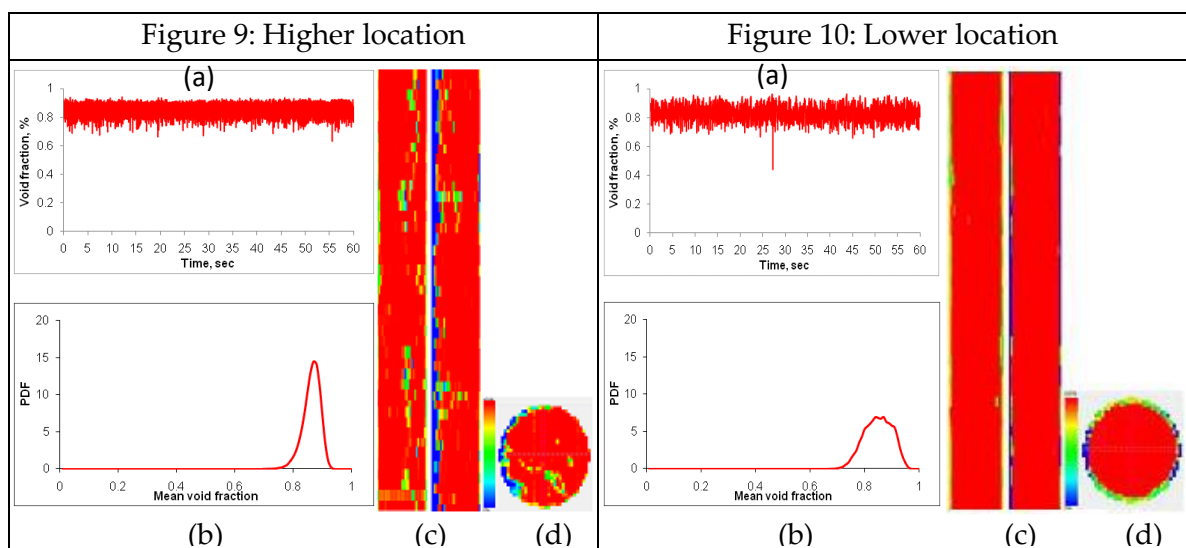
fraction. The action of the force led to create a huge oscillation in the mixture at the adjacent section of the bend (Figure 7 (a)). On the other hand, the identified flow type at the bottom location is slug (Figure 8 (a)). Analysis of PDF data at the top and bottom locations are also confirmed the results of time series. Figure 7 (b) shows flow instability accompanied by broad base of gas void fraction, for liquid and gas superficial velocities of 1.2 and 1.05 m/s, respectively. While, different structure of the flow regime (slug flow) is noted when it reached the bottom location of the pipe, as presented in Figure 8 (b). Again, the dissimilarity between the flow behavior at the higher and lower locations is due to the impact of the centrifugal force of the top bend on the distributions of void fraction. This impact is notably stronger at the adjacent section of the top bend and reduced when the flow reached the bottom of the pipe. Figure 7 (c) and (d) are respectively, presented the cross-sectional view and sliced stack images as another approach to validate the results of time traces and PDFs. Figure 7 (c) and (d) depicts the flow imaging at the top location which is an asymmetrically distributed and accompanied by a huge droplets of liquid. These droplets are entrained in the centre of the pipe in the form of wisps, due to the significant effect of centrifugal force. The force is noted to push the liquid phase on the inner wall of bend's outer curvature. The effect of force is reduced as the fluid reached the lower location of the pipe and less wisps can be observed, as illustrated in Figure 8 (c) and (d).



Figures 7 & 8: (a) Time traces, (b) PDF, (c) cross-sectional view and (d) sliced stack image of void fraction at higher and lower locations of downward orientation, for gas velocity=1.05 m/s and liquid velocity=1.2 m/s

Figures 9 (a) and 10 (a) respectively, represent the time traces at the top location of the pipe (close to the bend) and lower location (a part away from the top bend) for superficial gas velocity of 17.55 m/s and fixed liquid velocity=1.2 m/s. It can be seen

from Figure 9 (a) that there are extensive waves when compared with those identified at the lower location (i.e., Figure 10 (a)). The difference is attributed to the large amount of trapped bubbles in the centre of the pipe that located at the adjacent part of the top bend. Figures 9 (b) and 10 (b) represent the PDF characteristics of void fraction distributions at the top and bottom locations of the downward section, respectively. Both Figures show annular flow regime formation which is confirmed by sliced stack images and cross-sectional view. However, imaging of cross section and sliced stack at the top location of the downward section show considerable number of liquid droplets in the form of wisps at the pipe centre (Figure 9 (c) and (d)), This is due to centrifugal force that acting to expel the liquid into the outer curvature of the bend and creating a swirl flow in the straight sections. Figure 10 (c) and (d) shows that the annular flow became more stable and evenly distributed with almost no liquid entrainment when reached the bottom location of the downward orientation.

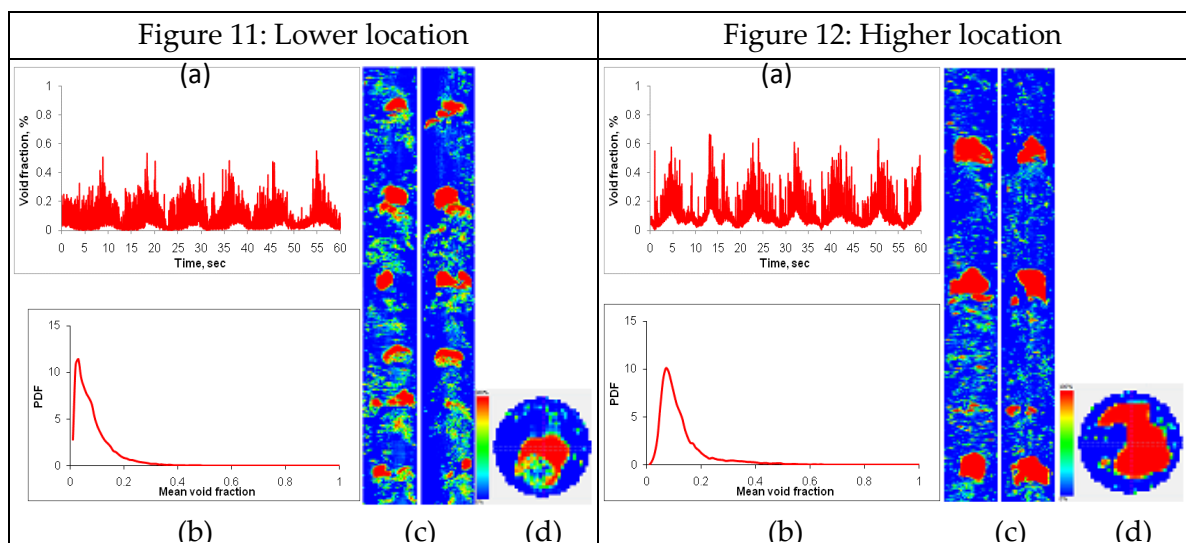


Figures 9 & 10: (a) Time traces, (b) PDF, (c) cross-sectional view and (d) sliced stack image of void fraction at higher and lower locations of downward orientation, for gas velocity=17.55 m/s and liquid velocity=1.2 m/s

3.2 Flow Structure Along Upward Section

Data of time traces, PDFs, cross-sectional view and sliced stack image of gas void fraction are presented in Figures 11 and 12. The experiments are conducted for gas velocity of 0.17 m/s, and fixed liquid velocity of 1.2 m/s. The time series data at lower location are quite different from those located at higher location, as shown in Figures 11 (a) and 12 (a), respectively. It can be noted that the maximum percentage of gas void fraction at a lower position is less than that at the higher part. However, the flowrates applied for both positions are the same. This can be attributed to the effect of bottom bend that lead to create a flow transition from bubbly to intermittent close

to the bend (i.e., bottom position), which means that the mixture structure is not developed yet. Vice versa, when the flow reached to higher position (far away from the bottom bend), the signal of time traces show different behavior due to reduction in the effect of bottom bend. This in turn led to stability in the mixture and create intermittent flow regime, as illustrated in Figure 12 (a). The data of time traces is confirmed by PDFs data, as presented in Figures 11 (b) and 12 (b). The PDF shape at the bottom position shows existence of large bubbles accompanied by broad base of void fraction. This indicates that the flow regime is still under transition from bubbly to intermittent, as illustrated in Figure 11 (b). On the other hand, the PDF shape confirms a development of the flow into an intermittent when the mixture reached the top section of the pipe, as presented in Figure 12 (b). To confirm the abovementioned results, further analysis is performed by cross-sectional view of the void fraction distribution and its sliced stack image, as shown in Figure 11 (c) and (d), respectively. It can be clearly observed that, the transition region from bubbly to intermittent flow is occurred at lower location. With growing distance from the bottom bend (at higher location), the bubbles started to colloid and coalesce with each other which became larger in their size having pullet shape. These bubbles are commonly known as Taylor bubbles, as depicted in Figure 12 (c) and (d).

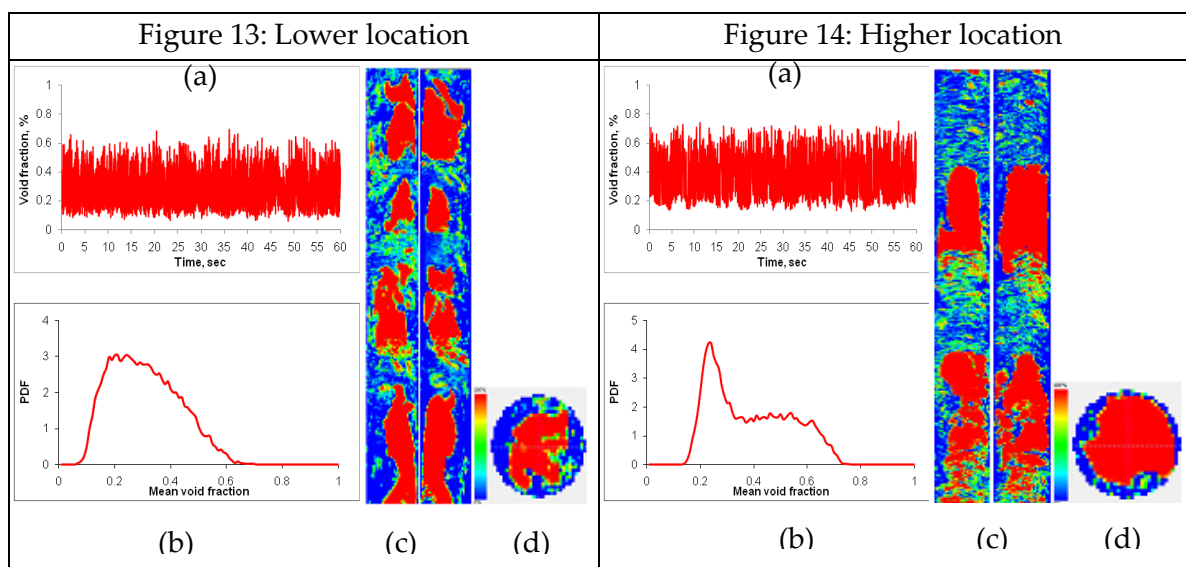


Figures 11 & 12: (a) Time traces, (b) PDF, (c) cross-sectional view and (d) sliced stack image of void fraction at lower and higher locations of upward orientation, for gas velocity=0.17 m/s and liquid velocity=1.2 m/s

When gas velocity increased to 1.05 m/s and liquid velocity=1.2 m/s, the bubbles colloid and coalesce together which became larger if compared with those formed by the previous gas velocity (i.e., by gas velocity of 0.17 m/s). The signal of time traces presented in Figure 13 (a) showed that, the flow regime is likely to be a

transition from bubbly to an intermittent accompanied by large oscillation of waves. Analysis of PDF at these flow conditions is also indicating a transition from bubbly to an intermittent flow having extended base of gas void fraction, as illustrated in Figure 13 (b). These observations are confirmed by the cross sectional view of averaged void fraction and corresponding sliced images, as can be seen in Figure 13 (c) & (d). It is very clear that the large bubbles are occupied a considerable part of a pipe centre accompanied by liquid droplets. This is because of the lower bend impact on flow structure in the near straight sections. The signal of time traces at the higher location presented in Figure 14 (a) shows an extensive waves with higher gas void fraction values when compared with the previous gas flowrate (namely, at gas velocity of 0.17 m/s). Double peaks are appeared in PDF shape which indicate to slug flow regime. The stability and development of the mixture when reached the higher position, resulted from reduction of the centrifugal force present in the bottom bend (Figure 14 (b)).

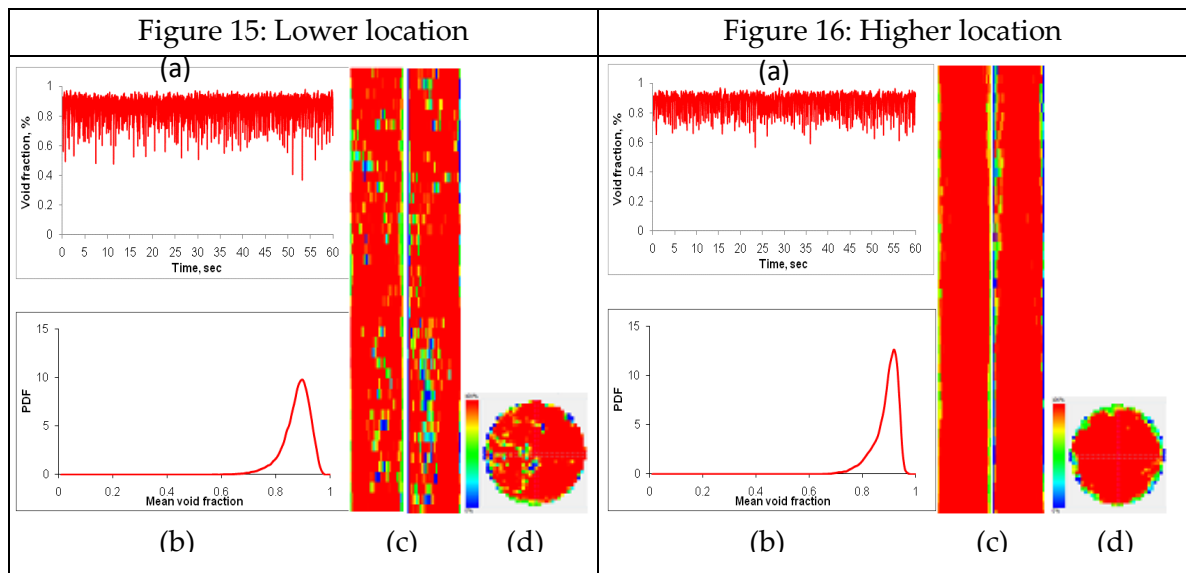
Figure 14 (c) and (d) validate the results of time traces and PDF, which can be noted that the flow is uniformly distributed in the cross-sectional area of the pipe with almost no entrained droplets. The cross-sectional view and sliced image depicted that the formed bubbles are larger in their size than those identified at the lower position.



Figures 13 & 14: (a) Time traces, (b) PDF, (c) cross-sectional view and (d) sliced stack image of void fraction at lower and higher locations of upward orientation, for gas velocity=1.05 m/s and liquid velocity=1.2 m/s

Figures 15 (a) and 16 (a) respectively, show similar behavior of time traces signals at the lower and higher positions of the test facility for superficial gas velocity of 17.55 m/s. Similarly, analysis of PDF data at these locations are to somehow identical in

their shape, as presented in Figures 15 (b) and 16 (b). The observed flow regime in both locations is annular accompanied by expansion in void fraction values. The centrifugal force generated by the bottom bend acts on the lower straight pipe, and therefore a huge number of liquid is entrained into the pipe centre in the form of droplets as a result. These observations are confirmed by cross-sectional view and sliced stack images, as illustrated in Figure 15 (c & d).



Figures 15 & 16: (a) Time traces, (b) PDF, (c) cross-sectional view and (d) sliced stack image of void fraction lower and higher locations of upward orientation, for gas velocity=17.55 m/s and liquid velocity=1.2 m/s

3.3 Circumferential Distribution of Liquid Film

Circumferential distribution of liquid film is investigated along different locations of the pipe in order to validate the above-mentioned results. In general, the data of circumferential distribution of liquid film are consistent with the PDF shapes and time traces signals. The film thickness profile close to the bottom bend is obviously affected by the action of generated centrifugal force. This impact is decreased when the flow reached the higher locations and uniform liquid film distribution around the cross section of the pipe is noted as a result.

Figures 17 and 18 are respectively, presented the circumferential distribution of liquid film at various locations of downward and upward flow line. The superficial gas velocities are 1.32 and 9.32 m/s, respectively, while liquid velocity is adjusted at 1.2 m/s.

3.3.1 Circumferential Profile of Liquid Film in Downward Flow

Figure 17 (a) and (b) shows the shape of liquid film at 90 degree of the higher location which is corresponding to CT2 sensor. This sensor is located in the outer side of the top bend. For the whole tested flowrates, the liquid film measured by sensor CT2 was notably thicker than those measured by the other sensors (namely, at 0°, 180° and 270°). This was attributed to the action of centrifugal force that acts to expel the liquid phase into 90 degree position of the bend's outer curvature. The impact of this force was reduced when the mixture became apart from the bend. This leads to identical profile of the liquid film at the middle and lower locations of the flow path. The liquid film at the middle and lower location of the downward section presented a similar characteristic even at higher flowrates. This means that the impact of the top bend is diminishes as the mixture reached the lower locations of the pipe (Figure 17 (b)).

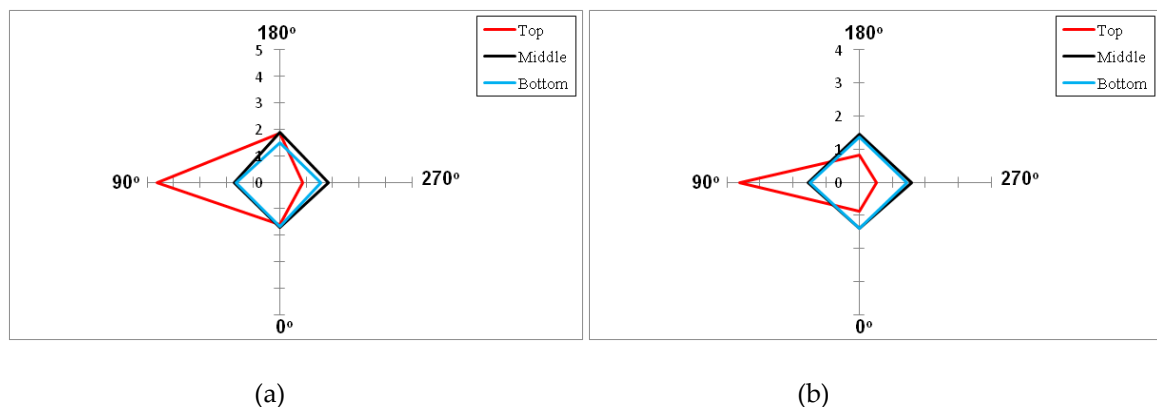


Figure17: Circumferential profile of the liquid film in downward location at gas velocities of 1.32 m/s (a) and 9.32 m/s (b), and liquid velocity of 1.2 m/s. (Axes unit in all plots is mm)

3.3.2 Circumferential Profile of Liquid Film in Upward Flow

For gas velocity of 1.32 m/s and liquid velocity of 1.2 m/s, uniform distribution of liquid film at higher, middle and lower locations of upward section along the flow path, as illustrated in Figure 18 (a). However, the liquid film obtained at the lower position is thicker than those obtained at the other positions. Asymmetrical circumferential distribution of liquid film is noted at lower location, with increasing gas velocity to 9.32 m/s (Figure 18 (b)). Furthermore, Figure 18 (b) also shows that the liquid film measured at 90° (namely at CT6) is thicker than those measured by the other sensors (i.e., by CT5, CT7 and CT8). This is attributed to the impact of centrifugal force generated by the lower bend and acting on CT6. It is worth mentioning that CT6 is located in the same position of the lower bend's outer curvature.

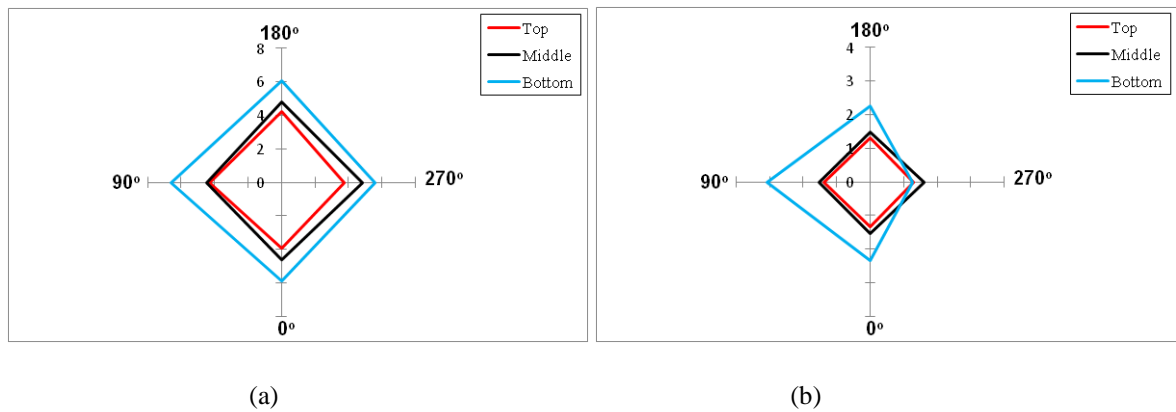


Figure 18: Circumferential profile of the liquid film in upward section at superficial gas velocities of 1.32 m/s (a) and 9.32 m/s (b), and superficial liquid velocity of 1.2 m/s. (Axes unit in all plots is mm)

4. Conclusions

- 1- Significant impacts of bends on gas void fraction and distribution of liquid are obviously observed at downward and upward sections of the pipeline, although to varying degree.
- 2- It can be seen from PDFs, time traces, cross-sectional view and sliced images that the gas flowrates play a vital role on development of gas void fraction and liquid film.
- 3- The characteristics of fluids flowing close to the bends are highly affected than those flowing apart away.
- 4- Bubbly, intermittent, slug and annular flow regimes are identified in this study.
- 5- The variations of flow regime along both orientations are attributed to the effect of applied velocities.
- 6- The fluctuation in the mixture is attributed to centrifugal force generated by the bends.
- 7- Finally, it can be concluded that the wire mesh sensor and liquid film probes are suitable techniques in identifying the bend impacts on the structure of two-phase fluids.

References

- [1] Abdulkadir, M., D. Zhao, Azzi, A., Lowndes, I. S. & Azzopardi, B. J., 2012. Two-phase air-water flow through a large diameter vertical 180° return bend. *Chemical Engineering Science*, **79**, pp. 138–152.
- [2] Alves, G.E., Co-current liquid-gas flow in a pipeline contactor, 1954. *Chemical Engineering Progress*, **50**, pp. 449–456.
- [3] Oshinowo, T. & Charles, M.E., 1974. Vertical two-phase flow—Part 1: Flow pattern correlations. *The Canadian Journal of Chemical Engineering*, **52**, pp. 25–35.
- [4] Usui, K., Aoki, S., & Inoue, A., 1983. Flow behaviour and phase distributions in two phase flow around inverted U-bend. *Journal of Nuclear Science and Technology*, **20**, pp. 915–928.
- [5] Azzi, A., Friedel, L., Kibboua, R. & Shannak, B., 2002. Reproductive accuracy of two-phase flow pressure loss correlations for vertical 90 degree bends. *Forschung im Ingenieurwesen*, **67**, pp. 109–116.
- [6] Azzi, A. & Friedel, L., 2005. Two-phase upward flow 90 degree bend pressure loss model. *Forschung im Ingenieurwesen*, **69**, pp. 120–130.
- [7] Spedding, P.L., & Benard, E., 2006. Gas-liquid two-phase flow through a vertical 90 degree elbow bend. *Experimental Thermal and Fluid Science*, **31**, pp. 761–769.
- [8] Shannak, B., Al-Shannag, M., & Al-Anber, Z. A., 2009. Gas-liquid pressure drop in vertically wavy 90° bend. *Experimental Thermal and Fluid Science*, **33**, pp. 340–347.
- [9] Da Silva, M.J., Thiele, S., Abdulkareem, L., Azzopardi, B.J., & Hampel, U., 2010. High resolution gas-oil two-phase flow visualization with a capacitance wire mesh sensor. *Flow Measurement and Instrumentation*, **21**, pp. 191–197.